RECOMMENDATION ITU-R S.1529

Analytical method for determining the statistics of interference between non-geostationary-satellite orbit fixed-satellite service systems and other non-geostationary-satellite orbit fixed-satellite service systems or geostationary-satellite orbit fixed-satellite service networks

(Question ITU-R 231/4)

(2001)

The ITU Radiocommunication Assembly,

considering

a) that emissions from the earth stations as well as from the space stations of satellite systems (geostationary-satellite orbit fixed-satellite service (GSO FSS), non-GSO FSS, non-GSO mobile-satellite service (MSS) feeder links) in the FSS may result in interference to another such system when both systems operate in the same frequency bands;

b) that when non-GSO satellite systems are involved, the statistical behaviour of interference, especially that related to short-term events, constitutes an important factor in interference evaluation studies;

c) that it is desirable to have reliable and precise tools for determining the statistical behaviour of interference between systems that have co-frequency links when the interference environment involves non-GSO satellite systems;

d) that computer simulation methods (see Recommendation ITU-R S.1325) may require an excessively long computer time to ensure that all interference events are taken into account and thus statistically significant results are obtained,

recommends

1 that the analytical method given in Annex 1 should be considered as a possible method for use in obtaining aggregate interference cumulative probability distributions for assessing the interference between systems that have co-frequency links when the interference environment involves non-GSO satellite systems.

ANNEX 1

An analytical method for assessing interference in interference environments involving non-GSO satellite systems

1 Introduction

Most of the existing methods to assess interference involving non-GSO satellite systems are based on direct computer simulation. These methods are usually time consuming and require a new lengthy simulation run each time a change is made in some of the system and system parameters. Also, in complex situations, involving a large number of earth stations and non-GSO satellites, these methods may require a very long computer time to produce statistically significant results. This Annex presents an analytical method, that can be implemented through numerical techniques, intended to perform the evaluation of interference sensitivity to system and system parameters without requiring lengthy computer simulation runs. Also, as opposed to results generated through simulation, the results obtained with the analytical approach correspond to an infinite number of simulated days, and therefore, in this sense, they do not present the need for long running times, as may be required in computer simulation methods to assure statistically significant results.

The method is based on the knowledge of the probability density function (pdf) of the position of a single satellite placed in an orbit with an arbitrary inclination. To illustrate the applicability of the proposed method to complex interference environments, results for some specific situations are presented. Comparisons of the results obtained using the proposed method and those generated by a widely used commercially available simulation software have indicated that the proposed method can generate reliable and precise results with less required computer time.

2 Methodology

Let us consider an interference environment involving several, say n, non-GSO systems. The approach being considered in this Recommendation to assess interference in such an environment takes into account the fact that, once the position of one particular satellite (here referred to as reference satellite) in each constellation is known, the aggregate interference levels affecting the receivers of any interfered-with system in the environment (considering that all systems parameters are given) can be uniquely determined. It further assumes that the positions of these reference satellites are characterized by statistically independent random vectors. Based on these assumptions, desired and interfering signal power levels can be seen as random variables that are deterministic functions of the positions of the reference satellites, and therefore their pdf's can be determined once the pdf's modelling the positions of each of the n reference satellites are known.

As an example, consider the situation illustrated in Fig. 1. This Figure shows two non-GSO satellite systems, both having circular orbits and arbitrary satellite constellations. Satellites of system 1 move on surface E_1 and satellites of system 2 move on surface E_2. Reference satellites for both systems are also indicated. In this example the downlink aggregate interference from system 1 satellites into a given earth station in system 2 is considered. Given that reference satellite S_i of system i ($i = 1, 2$) is located at longitude φ_i and latitude θ_i the positions of all other satellites in both constellations can be uniquely determined as a function of the two location vectors $\mathbf{x}_1 = (\varphi_1, \theta_1)^T$ and $\mathbf{x}_2 = (\varphi_2, \theta_2)^T$. Therefore, considering for instance that the earth station antenna always points to the nearest satellite in the constellation of its system, and that all other systems parameters, such as satellite and earth station antenna radiation patterns, e.i.r.p., etc. are known, then both the downlink aggregate interference I and the desired signal level C at the considered earth station can be computed for each pair of values of the vectors $\mathbf{x}_i = (\varphi_i, \theta_i)^T$, $-\pi < \varphi \leq \pi, -\delta_i \leq \theta_i \leq \delta_i$, where $i = 1, 2$ (δ_i is the angle between the equatorial plane and the plane containing the orbit of S_i). If these two vectors are modelled as statistically independent random vectors with known pdf's

$p_{\mathbf{x}_i}(\Phi,\Theta), i = 1, 2$ then the desired signal level $C(\mathbf{x}_1,\mathbf{x}_2)$ and the aggregate interference $I(\mathbf{x}_1,\mathbf{x}_2)$ correspond to random variables whose statistical characterization, e.g. pdf or cumulative distribution function (CDF), can be obtained from $p_{\mathbf{x}_i}(\Phi,\Theta), i = 1, 2$ through analytical and/or numerical methods.

FIGURE 1

Interference environment involving two non-GSO satellite systems

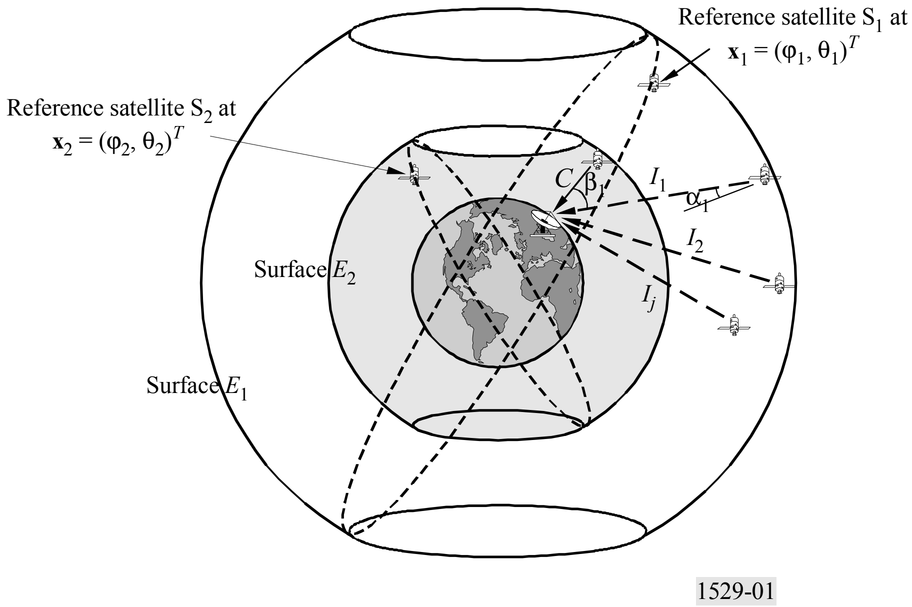

The pdf $p_{\mathbf{x}}(\Phi,\Theta)$ of the position (longitude and latitude) of a satellite placed in elliptical orbit around the Earth can be shown to be (see Appendix 1 to this Annex):

$$p_{\mathbf{x}}(\Phi,\Theta) = p_{\mathbf{x}|AM}(\Phi,\Theta)P(AM) + p_{\mathbf{x}|DM}(\Phi,\Theta)P(DM) \tag{1}$$

where $p_{\mathbf{x}|AM}(\Phi,\Theta)$ and $p_{\mathbf{x}|DM}(\Phi,\Theta)$ are the pdf's of the satellite position (longitude and latitude) given that the satellite is in ascending and descending mode, respectively. These conditional pdf's are given by:

$$p_{\mathbf{x}|AM}(\Phi,\Theta) = \begin{cases} \dfrac{1}{P(AM)} \dfrac{k(1+e)}{4\pi^2} \dfrac{\cos\Theta}{\sqrt{\sin^2\delta - \sin^2\Theta}} \left[\dfrac{2\sin\delta}{(1+k^2)\sin\delta - (1-k^2)g(\Theta)}\right]^2 & \text{for } -\delta < \Theta \le \delta \\ & \quad -\pi < \Phi \le \pi \\ 0 & \text{otherwise} \end{cases} \tag{2}$$

and

$$p_{\mathbf{x}|DM}(\Phi,\Theta) = \begin{cases} \dfrac{1}{P(DM)} \dfrac{k(1+e)}{4\pi^2} \dfrac{\cos\Theta}{\sqrt{\sin^2\delta - \sin^2\Theta}} \left[\dfrac{2\sin\delta}{(1+k^2)\sin\delta + (1-k^2)g(-\Theta)}\right]^2 & \text{for } -\delta < \Theta \le \delta \\ & \quad -\pi < \Phi \le \pi \\ 0 & \text{otherwise} \end{cases} \tag{3}$$

with $P(AM)$ and $P(DM)$ given by equations (60) and (61).

Note that equation (1) can be also written as:

$$p_{\mathbf{x}}(\Phi,\Theta) = \begin{cases} \dfrac{k(1+e)}{4\pi^2} \dfrac{\cos\Theta}{\sqrt{\sin^2\delta - \sin^2\Theta}} \left[\left(\dfrac{2\sin\delta}{(1+k)\sin\delta - (1-k^2)g(\Theta)} \right)^2 + \left(\dfrac{2\sin\delta}{(1+k)\sin\delta + (1-k^2)g(-\Theta)} \right)^2 \right] & \text{for } -\delta < \Theta \le \delta \\ & \quad -\pi < \Phi \le \pi \\ 0 & \text{otherwise} \end{cases} \tag{4}$$

In equations (2), (3) and (4), δ is the angle between the orbital plane and the equatorial plane,

$$k = \sqrt{\frac{1+e}{1-e}} \tag{5}$$

with e denoting the orbit eccentricity, and

$$g(\Theta) = \cos\omega\sqrt{\sin^2\delta - \sin^2\Theta} + \sin\omega\sin\Theta \tag{6}$$

where ω is the argument of the perigee.

In the particular case of circular orbits ($e = 0 \rightarrow k = 1$), equation (1) is reduced to:

$$p_{\mathbf{x}}(\Phi,\Theta) = \begin{cases} \dfrac{1}{2\pi^2} \dfrac{\cos\Theta}{\sqrt{\sin^2\delta - \sin^2\Theta}} & \text{for } -\delta < \Theta < \delta \\ & \quad -\pi < \Phi \le \pi \\ 0 & \text{otherwise} \end{cases} \tag{7}$$

This pdf is illustrated in Fig. 2 for a satellite in a circular orbit on a plane inclined 45° with respect to the equatorial plane.

FIGURE 2

pdf p_x (Φ, Θ) of the position of a satellite placed in a circular orbit on a plane inclined 45° with respect to the equatorial plane

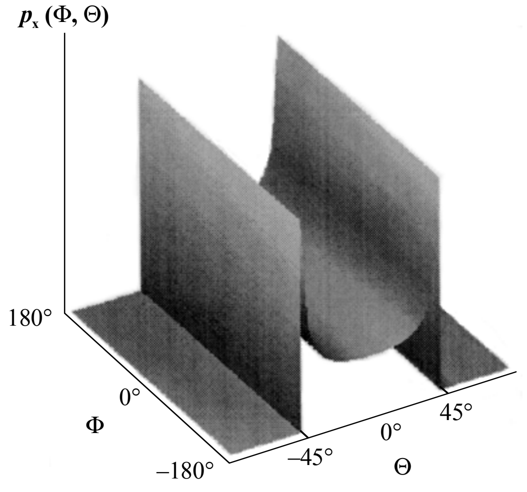

1529-02

3 Procedure to obtain the interference CDF

For simplicity, let us assume that only a single non-GSO system is involved in the interference environment. The longitude and latitude of the reference satellite of this non-GSO satellite system takes values on a φ-θ plane ($-\pi < \varphi \le \pi, -\delta \le \theta \le \delta$). In a first step, this plane is finely partitioned into small rectangular cells. For each of these partition cells, it is assumed that the reference satellite is located at its centre and, for this condition, the position of all other satellites in the constellation are determined. We note that there are two possible constellation configurations associated with a given position of the reference satellite: one corresponding to the satellite in ascending mode and another for the satellite in descending mode – both situations have to be taken into account. For each of the two constellation configurations, once the position of all satellites are known, the aggregate interference level into the desired test point is evaluated. To generate the probability distribution of a quantized version of the aggregate interference, the two obtained values (ascending mode and descending mode) are quantized to the nearest quantization levels and the corresponding probabilities of finding the reference satellite inside the considered cell, obtained using equations (2) and (3), are added to the current values of probability associated to the two corresponding quantization levels. This procedure is then repeated for all partition cells and the so obtained histogram is integrated to generate the desired CDF. The flowchart in Fig. 3 illustrates the procedure described above.

Concerning this procedure, the following additional comments are pertinent:

– Although the partition of the φ-θ plane into rectangular cells need not be a grid-type of partition, the use of grid-type partitions is convenient for implementation purposes. However, to avoid a prohibitive amount of required computer time when applying the proposed analytical method to complex situations involving a large number of earth stations and satellites, the following points should be taken into account:

  – The φ-θ plane quantization grid should be sufficiently fine to detect fast variations of the interference levels that occur near to "in-line" interference situations. However, a fine quantization of the whole φ-θ plane could result in an excessively large computer time. So, the numerical implementation of the analytical method could, as an option, be split in two parts. The first part performs the calculations in the regions of the φ-θ plane for which the interference level may have large variations (close to in-line interference), and where a fine quantization of the region is required. The second part of the numerical procedure performs the calculations in the regions of the φ-θ plane for which the interference level has smooth variations, allowing for a coarser quantization. Finding the φ-θ plane regions associated with potential quasi "in-line" interference corresponds to defining regions such that when the reference satellite is inside one of these regions, in-line interference events involving one or more of the satellites in the constellation may occur. The important point here is to guarantee that when the reference satellite is not inside any of these regions, "in-line" interference does not occur and a coarser quantization grid can be used. The regions of potential in-line interference (**RPII**) are usually defined as rectangular regions around points of potential in-line interference (**PPII**). These **PPII** can be found using the methodology described in Section 6.

  – Once the potential occurrence of quasi in-line interference is detected (the reference satellite is inside one of the potential in-line interference regions), it is important to identify which satellites and earth stations are involved in it. This way interference computations could be made considering that only a few interference entries (those associated with the in-line interference event) have to be re-computed when the reference satellite changes its location inside the considered potential in-line interference region. This measure could save a substantial amount of computer time when a large number of interference entries are present.

FIGURE 3

Flow chart of the analytical method

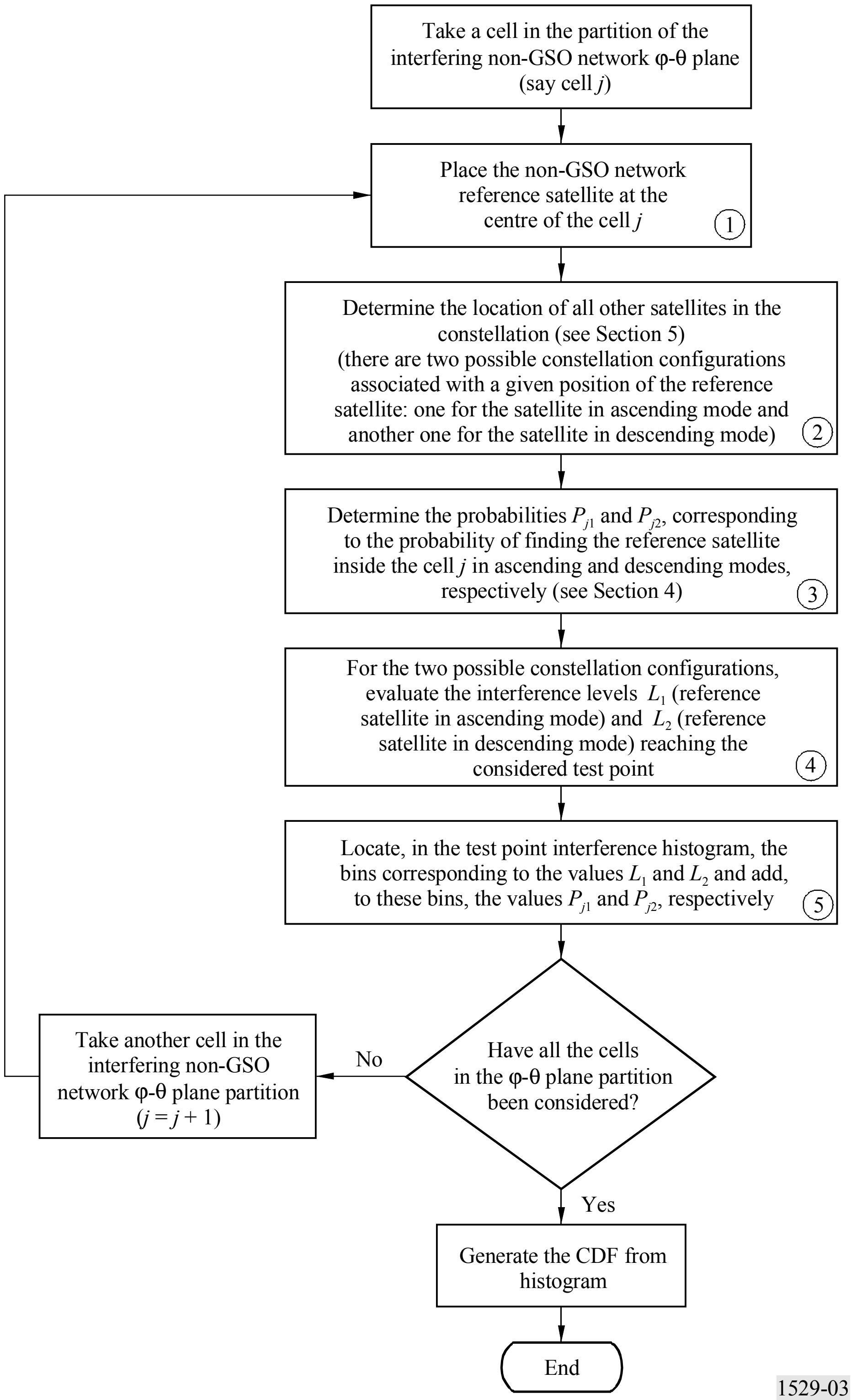

– Given the position of the reference satellite, finding the position of all other satellites in the constellation (block ③ in the diagram in Fig. 3) is a problem that has two possible solutions. This is due to the fact that two different orbital planes, having the same inclination, can contain the reference satellite. In fact, one of the solutions assumes that the reference satellite is in ascending mode and the other assumes that the reference satellite is in descending mode. Both solutions have to be taken into account in the proposed procedure. In the case of circular orbits, finding these solutions does not constitute a complex task, since the altitude of the satellites is previously known. For satellites in elliptical orbits, this is a more complex procedure, since the satellite altitudes change with time (see Section 5).

4 Probabilities of having the reference satellite inside a rectangular cell and in ascending and descending modes

Let a rectangular cell in the φ-θ plane, say cell *j*, be defined by $\varphi \in (\varphi_m, \varphi_M)$, $\theta \in (\theta_m, \theta_M)$. Also, let P_{j1} and P_{j2} represent respectively the probability of finding the reference satellite inside the rectangular cell *j* and in ascending mode, and the probability of finding the reference satellite inside the rectangular cell *j* and in descending mode. These two probabilities can be obtained by respectively integrating the two terms in the right hand side of equation (1), considering the values of *P*(*AM*) and *P*(*DM*) calculated through equations (60) and (61). It then results:

$$P_{jn} = \frac{\varphi_M - \varphi_m}{2\pi}\left[f\left(c_M,\ (n-1)\pi - (-1)^n \omega\right) - f\left(c_m, (n-1)\pi - (-1)^n \omega\right)\right] \qquad \text{for} \quad n = 1, 2 \tag{8}$$

with:

$$f(x,\omega) = \begin{cases} 0 & \text{for} \quad -\infty < x \le -\pi \\ Q_{ek}\left(\dfrac{x-\omega}{2}\right) - Q_{ek}\left(\dfrac{-\pi-\omega}{2}\right) & \text{for} \quad -\pi < x \le \pi \\ 1 & \text{for} \quad \pi < x < \infty \end{cases} \tag{9}$$

where:

$$Q_{ek}(x) = \frac{1}{\pi}\ \arctan\left(\frac{\tan(x)}{k}\right) + \frac{1}{2}\left[\operatorname{sgn}\left(x + \frac{\pi}{2}\right) + \operatorname{sgn}\left(x - \frac{\pi}{2}\right)\right] - \frac{k\,e}{\pi}\ \frac{\tan(x)}{\tan^2(x) + k^2} \tag{10}$$

with sgn( ) denoting the signum function. In equation (8),

$$c_m = \arcsin\left(\frac{\sin\theta_m}{\sin\delta}\right) \tag{11}$$

and

$$c_M = \arcsin\left(\frac{\sin\theta_M}{\sin\delta}\right) \tag{12}$$

In the case of circular orbits, since $\omega = 0$ and $e = 0 \rightarrow k = 1$, equation (9) is reduced to:

$$f(x,0) = \begin{cases} 0 & \text{for} \quad -\infty < x \le -\pi \\ \dfrac{1}{2}\left(1 + \dfrac{x}{\pi}\right) & \text{for} \quad -\pi < x \le \pi \\ 1 & \text{for} \quad \pi < x \le \infty \end{cases} \tag{13}$$

5 Finding the position of all satellites in the constellation

In this section, the following notations and definitions are used.

$\mathbf{u}$	Unitary vector in the direction of the reference satellite
δ	Orbit inclination angle (rad)
β	Satellite separation angle within the orbital plane (in terms of mean anomaly) (rad)
ψ	Angle between the intersections of adjacent orbit planes and the equatorial plane (rad)
λ	Satellite phasing between planes (rad)
r	Orbit radius (circular orbit) (km)
a	Major semi-axis of the elliptical orbit (km)
e	Orbit eccentricity
ω	Argument of the perigee (rad)
$\mathbf{k}_z$	Unitary vector in the z-axis direction
γ_ℓ	True anomaly of the reference satellite in constellation configuration ℓ measured from the line of nodes (rad)
υ_ℓ	True anomaly of the reference satellite in constellation configuration ℓ (rad)
E_ℓ	Eccentric anomaly of the reference satellite in constellation configuration ℓ (rad)
M_ℓ	Mean anomaly of the reference satellite in constellation configuration ℓ (rad)
$(M_i^j)_\ell$	Mean anomaly of the *i*-th satellite in the *j*-th orbital plane, corresponding to constellation configuration ℓ (rad)
$(E_i^j)_\ell$	Eccentric anomaly of the *i*-th satellite in the *j*-th orbital plane, corresponding to constellation configuration ℓ (rad)
$J_n(\cdot)$	Bessel Function of first class and order *n*
$(\upsilon_i^j)_\ell$	True anomaly of the *i*-th satellite in the *j*-th orbital plane, corresponding to constellation configuration ℓ (rad)
$(\mathbf{u}_i^j)_\ell$	Unitary vector in the direction of the *i*-th satellite in the *j*-th orbital plane, corresponding to constellation configuration ℓ
$(\mathbf{p}_i^j)_\ell$	Vector of the position of the *i*-th satellite in the *j*-th orbital plane, corresponding to constellation configuration ℓ
$(r_i^j)_\ell$	Distance, from the centre of the Earth, of the *i*-th satellite in the *j*-th orbital plane, corresponding to constellation configuration ℓ (km)
$N_{Satperplane}$	Number of satellites per orbital plane
N_{Planes}	Number of orbital planes in the constellation

Consider a geocentric, GSO system of rectangular coordinates in which the x and y axis belong to the equatorial plane and the z-axis points to the north. Let $\mathbf{u}$ denote the unitary vector pointing to the reference satellite location and $(\mathbf{p}_i^j)_\ell$ be the vector characterizing the position of the *i*-th satellite in the *j*-th orbital plane, corresponding to constellation configuration $\ell, \ell = 1, 2$. The following procedure can be used to determine the locations $(\mathbf{p}_i^j)_\ell$ $(i = 0,\ldots, N_{Satperplane} - 1,$ $j = 0,\ldots, N_{Planes} - 1, \ell = 1, 2)$ of all satellites in the two constellation configurations. The described procedure includes a test to identify which of the two configurations corresponds to the reference satellite being in ascending mode and which corresponds to the reference satellite being in descending mode, as required by the proposed analytical method.

Step 1: Let $\mathbf{u} = (u_x, u_y, u_z)^T$ and calculate, for $\ell = 1, 2,$ the unitary vectors $\mathbf{n}_\ell$ defined by:

$$\mathbf{n}_\ell = \begin{pmatrix} (-u_z \cos\delta - a_\ell u_y)/u_x \\ a_\ell \\ \cos\delta \end{pmatrix} \tag{14}$$

with

$$a_\ell = \frac{-u_y u_z \cos\delta + (-1)^\ell u_x \sqrt{(u_x^2 + u_y^2)\sin^2\delta - u_z^2 \cos^2\delta}}{u_x^2 + u_y^2}$$

Step 2: Let $\mathbf{k}_z$ be the unitary vector in the z-axis direction and calculate the following quantities for $\ell = 1, 2$:

$$\mathbf{w}_\ell = \mathbf{k}_z \times \mathbf{n}_\ell \quad (\times \text{denotes the cross product})$$

$$\gamma_\ell = \arccos\left(\frac{\mathbf{u}^T \mathbf{w}_\ell}{|\mathbf{w}_\ell|}\right)\operatorname{sgn}(u_z) \tag{15}$$

(T denotes transpose and sgn( ) denotes the signum function)

$$\upsilon_\ell = (\gamma_\ell - \omega)_{MOD\ 2\pi}$$

(throughout this Annex, $(x)_{MOD\ 2\pi}$ is defined in the interval $(-\pi, \pi)$)

$$E_\ell = 2\arctan\left(\frac{\tan(\upsilon_\ell / 2)}{k}\right)$$

where $k = \sqrt{\dfrac{1+e}{1-e}}$

$$M_\ell = E_\ell - e\sin E_\ell$$

$$(M_i^j)_\ell = M_\ell + i\beta + j\lambda \tag{16}$$

$$(E_i^j)_\ell = (M_i^j)_\ell + 2\sum_{n=1}^{\infty} \frac{1}{n} J_n(ne)\sin\left(n(M_i^j)_\ell\right)$$

$$(\upsilon_i^j)_\ell = 2\arctan\left(k\ \tan\frac{(E_i^j)_\ell}{2}\right)$$

$$(\alpha_i^j)_\ell = (\upsilon_i^j)_\ell - \upsilon_\ell$$

Note that the quantity β in equation (16) is usually given by:

$$\beta = \frac{2\pi}{N_{Satperplane}}$$

Important Note: The values of γ_ℓ determined through equation (15) are used to identify which of the two configurations corresponds to the reference satellite being in ascending mode and which corresponds to the reference satellite being in descending mode. This is accomplished by the following test:

$$\begin{cases} \text{if} \quad 0 \le |\gamma_\ell| < \pi/2 & \rightarrow \quad \text{configuration } \ell \text{ corresponds to reference satellite in ascending mode} \\ \text{if} \quad \pi/2 \le |\gamma_\ell| \le \pi & \rightarrow \quad \text{configuration } \ell \text{ corresponds to reference satellite in descending mode} \end{cases} \tag{17}$$

Step 3: Determine the location vectors of the satellites in the two constellation configurations by:

$$(\mathbf{p}_i^j)_\ell = (r_i^j)_\ell \, (\mathbf{u}_i^j)_\ell$$

where:

$$(r_i^j)_\ell = \frac{a(1-e^2)}{1 - e\cos\left((\upsilon_i^j)_\ell\right)}$$

and

$$(\mathbf{u}_i^j)_\ell = \cos((\alpha_i^j)_\ell)\, \mathbf{M}_j \, \mathbf{u} - \sin((\alpha_i^j)_\ell)\, \mathbf{M}_j \, \mathbf{b}_\ell$$

with:

$$\mathbf{b}_\ell = \mathbf{u} \times \mathbf{n}_\ell$$

and

$$\mathbf{M}_j = \begin{pmatrix} \cos j\psi & -\sin j\psi & 0 \\ \sin j\psi & \cos j\psi & 0 \\ 0 & 0 & 1 \end{pmatrix}$$

The angle ψ is usually given by:

$$\psi = \frac{2\pi}{N_{Planes}}$$

In the particular case of circular orbits, since the true anomaly, the eccentric anomaly and the mean anomaly are all the same, and since $a = r$ and $e = 0 \rightarrow k = 1$, Steps 2 and 3 simplify to:

Step 2:

$$(\alpha_i^j)_\ell = i\beta + j\lambda$$

Step 3:

$$(\mathbf{p}_i^j)_\ell = r\,(\mathbf{u}_i^j)_\ell$$

where:

$$(\mathbf{u}_i^j)_\ell = \cos((\alpha_i^j)_\ell)\, \mathbf{M}_j \, \mathbf{u} - \sin((\alpha_i^j)_\ell)\, \mathbf{M}_j \, \mathbf{b}_\ell$$

with:

$$\mathbf{b}_\ell = \mathbf{u} \times \mathbf{n}_\ell$$

and

$$\mathbf{M}_j = \begin{pmatrix} \cos j\psi & -\sin j\psi & 0 \\ \sin j\psi & \cos j\psi & 0 \\ 0 & 0 & 1 \end{pmatrix}$$

6 Choosing the longitude and latitude increments for the fine and coarse grids

The φ-θ plane quantization grid should be sufficiently fine to detect fast variations of the interference levels that occur near to in-line interference situations. However, a fine quantization of the whole φ-θ plane could result in an excessively large computer time. So, the numerical implementation of the analytical method can, as an option, be split in two parts. The first part performs the calculations in the regions of the φ-θ plane in which the interference level may have large variations (close to in-line interference), and where a fine quantization of the region is required. These regions are referred here as **RPII**. The second part of the numerical procedure performs the calculations in the regions of the φ-θ plane in which the interference level has smooth variations, allowing for a coarser quantization. It is suggested that the longitude and latitude increments $\Delta\varphi_f$ and $\Delta\theta_f$ for the fine grid be chosen such that:

$$\Delta\varphi_f \le \frac{\varphi}{10} \text{ and } \Delta\theta_f \le \frac{\varphi}{10} \tag{18}$$

For downlink interference calculations, φ in equation (18) is the geocentric angle defined by:

$$\varphi = \frac{1}{2}\varphi_{3dB} - \arcsin\left(\frac{R_{Earth}}{R_{Earth}+h}\sin\left(\frac{\varphi_{3dB}}{2}\right)\right) \tag{19}$$

where:

R_{Earth}: Earth radius

h: maximum orbit altitude

φ_{3dB}: 3 dB beamwidth (degrees) of the victim earth station antenna.

For uplink interference calculations, φ is also given in equation (19), with φ_{3dB} being the the 3 dB beamwidth (degrees) of the interfering earth station antennas.

For inter-satellite interference calculations (a lower orbit satellite passing through the main beam of the victim higher orbit satellite), φ in equation (18) is the geocentric angle defined by:

$$\varphi = \arctan\left(2\sqrt{1-\left(\frac{R_{Earth}}{R_{Earth}+h}\right)^2}\left[\frac{R_{Earth}+H}{R_{Earth}+h}\sqrt{1-\left(\frac{R_{Earth}}{R_{Earth}+H}\right)^2}-\sqrt{1-\left(\frac{R_{Earth}}{R_{Earth}+h}\right)^2}\right]\sin\left(\frac{\varphi_{3dB}}{2}\right)\right) \tag{20}$$

where:

R_{Earth}: Earth radius

h: lower maximum orbit altitude

H: higher maximum orbit altitude

φ_{3dB}: 3 dB beamwidth (degrees) of the victim satellite antenna.

The longitude and latitude increments $\Delta\varphi_c$ and $\Delta\theta_c$ for the coarse grid should be chosen as:

$$\Delta\varphi_c = 1.5\varphi \text{ and } \Delta\theta_c = 1.5\varphi$$

with φ given by equation (19) for uplink and downlink interference calculations and by equation (20) for inter-satellite interference calculations.

Finding the φ-θ plane regions associated with potential quasi in-line interference corresponds to defining regions such that when the reference satellite is inside one of these regions in-line interference events involving one or more of the satellites in the constellation may occur. The important point here is to guarantee that when the reference satellite is not inside any of these regions, in-line interference does not occur and a coarser quantization grid can be used. The **RPII** are defined as regions (usually rectangular) around **PPII**. These **PPII** can be determined using the methodology described in Section 7. It is suggested that the **RPII** be defined by a $\Delta \times \Delta$ degree square region around the **PPII**s, where:

$$\Delta = 5\varphi$$

with φ given by equation (19) for uplink and downlink interference calculations and by equation (20) for inter-satellite interference calculations.

Although the above-mentioned values for the longitude and latitude increments as well as the size of the **RPII** were shown to be adequate in several exercises, they may have to be adjusted. Very large earth station (with very narrow beams) would require a decrease in the latitude and longitude increment size, but would allow for a smaller **RPII**. On the other hand, earth stations with a broad beam would allow for larger values of the longitude and latitude increments, but would require a larger **RPII**.

7 Finding the PPII

In the case that the optional fine grid is used then the following points are to be noted:

7.1 Uplink interference

For each GSO interfered-with satellite (test point), the following steps should be used in determining the **PPII** in the case of uplink interference calculations:

Step 1: For each interfering non-GSO system earth station, identify the position of the interfering system satellite that is in line with the considered earth station and the GSO interfered-with satellite.

Step 2: Place the reference satellite at this position and determine the position of all other satellites in the constellation for the two possible configurations, according to Section 5.

Step 3: These $N_{non\text{-}GSOearthstation} \times N_{non\text{-}GSOsatellites} \times 2$ satellite positions form the set of **PPII**s.

It should be noted that the switch-off algorithm should ensure that the non-GSO earth station does not transmit towards non-GSO satellites that are in the exclusion zone, and so the use of the fine grid for the uplink may not be necessary.

7.2 Downlink interference

For each GSO system interfered-with earth station (test point), the following steps should be used in determining the **PPII** in the case of downlink interference calculations:

Step 1: Identify the position of the interfering system satellite that is in line with the considered interfered with GSO system earth station (test point) and the GSO satellite serving it.

Step 2: Place the reference satellite at this position and determine the position of all other satellites in the constellation for the two possible configurations, according to Section 5.

Step 3: These $N_{non\text{-}GSOsatellites} \times 2$ satellite positions form the set of **PPII**s.

7.3 Inter-satellite interference

For each GSO interfered-with satellite (test point), the following steps should be used in determining the **PPII** in the case of inter-satellite interference calculations:

Step 1: Let $N_{GSOsatellitebeams}$ denote the number of co-frequency beams in the interfered-with GSO satellites being considered. For each of these beams, identify the position of the interfering non-GSO satellite that is on the beam axis.

Step 2: Place the reference satellite at this position and determine the position of all other satellites in the constellation for the two possible configurations, according to Section 5.

Step 3: These $N_{GSOsatellitebeams} \times N_{non\text{-}GSOsatellites} \times 2$ satellite positions form the set of **PPII**s.

8 Additional use of fine grids

Fast variations of interference can also occur when satellites approach the boundary line that characterizes the exclusion angle zone in the (regions of the φ-θ plane where the non-GSO satellites do not operate). In the vicinity of this boundary line (exclusion zone vicinity regions (**EZVR**s)), fine grids could be also used to better detect these fast variations. The following steps should be used to determine these **EZVR**s:

Step 1: Determine, in the coarse grid, which cells contain the exclusion zone boundary curve. Let us say that the number of cells satisfying this condition is N_{EZ}.

Step 2: For each of these N_{EZ} cells, place the reference satellite at its centre and determine the position of all other satellites in the constellation for the two possible configurations, according to Section 5, and identify the coarse grid cells containing them.

Step 3: These $N_{EZ} \times N_{non\text{-}GSOsatellites} \times 2$ coarse grid cells will constitute the set of coarse grid cells inside which a finer grid is to be used.

9 Numerical examples

Two examples of the application of the analytical method are presented. Example 1 refers to the downlink aggregate interference from all satellites in a non-GSO system into a GSO system earth station. Results are also compared to those obtained with a widely used commercially available simulation software. Example 2 illustrates the applicability of the proposed methodology to an even more complex situation involving the uplink aggregate interference from a large number of non-GSO system earth stations (each with multiple beams) into a satellite located at a fixed point in the sky. Most of the data used in the examples were taken from Recommendation ITU-R S.1328, except those explicitly indicated in the following examples.

Example 1

This first example considers the downlink aggregate interference from all ten low Earth orbit (LEO) F satellites into an earth station of a GSO system, located at longitude 0° and latitude 30° N, pointing to a GSO satellite located at longitude 0º. This situation is illustrated in Fig. 4.

FIGURE 4

Downlink interference geometry

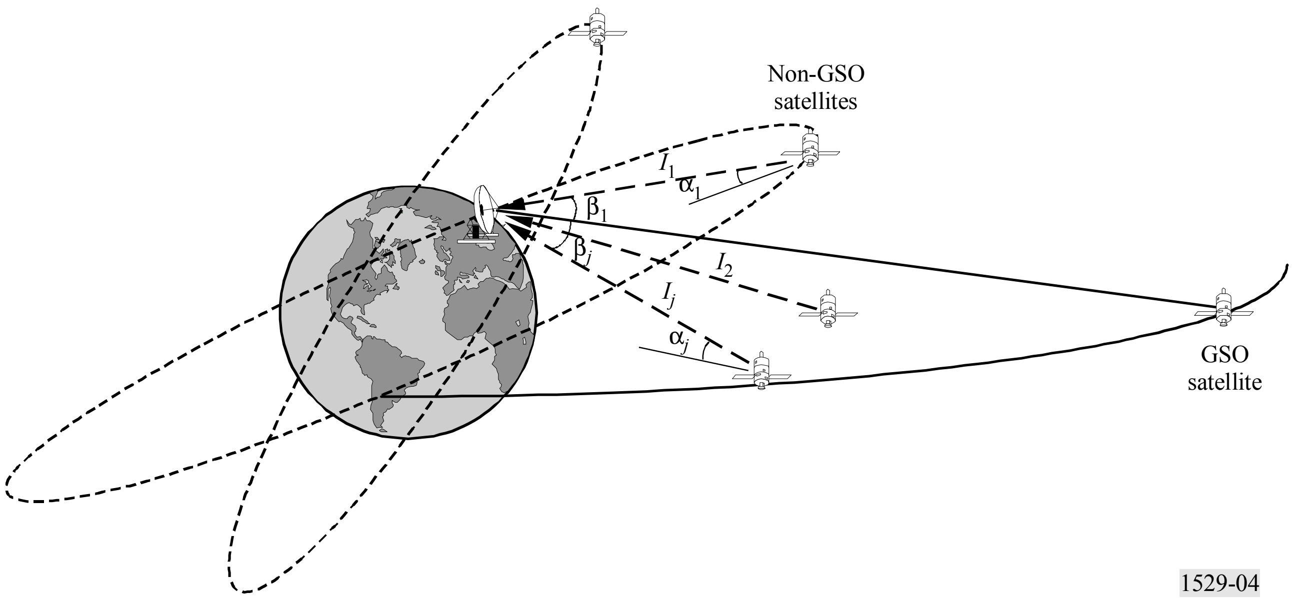

The earth station antenna radiation pattern was assumed to be:

$$G_e(\beta) = \begin{cases} 47.5 - 26.8177\,\beta^2 & \text{for} \quad 0^\circ \leq \beta \leq 0.76025^\circ \\ 32 & \text{for} \quad 0.76025^\circ < \beta \leq 1^\circ \\ 32 - 25\log\beta & \text{for} \quad 1^\circ < \beta \leq 48^\circ \\ -10 & \text{for} \quad 48^\circ < \beta \leq 180^\circ \end{cases}$$

corresponding to the pattern in Recommendation ITU-R S.465, for an antenna diameter equal to 6 m and a frequency of 5.175 GHz. The non-GSO satellite antenna radiation patterns (for all satellites) was assumed to be:

$$G_s(\alpha) = \begin{cases} G_{max} - 12\left(\dfrac{\alpha}{\alpha_0}\right)^2 & \text{for} \quad 0 \le \dfrac{\alpha}{\alpha_0} < 1.45 \\ G_{max} - \left(22 + 20\log\left(\dfrac{\alpha}{\alpha_0}\right)\right) & \text{for} \quad 1.45 \le \dfrac{\alpha}{\alpha_0} \end{cases}$$

with $G_{max} = 13$ dBi and $\alpha_0 = 52°$. This corresponds to the pattern in Appendix 30B to the Radio Regulations.

Assuming that all satellites transmit the same power, the downlink aggregate interference power reaching the earth station receiver is proportional to the quantity:

$$z = \sum_{i=1}^{10} \frac{G_{s,i}(\alpha_i)\, G_e(\beta_i)}{d_i^2}$$

where:

$G_{s,i}(\alpha_i)$: i-th non-GSO satellite transmitting antenna gain in a direction α_i (degrees) off the main beam axis

$G_e(\beta_i)$: GSO system earth station receiving antenna gain in a direction β_i (degrees) off the main beam axis

d_i: range between satellite i and the interfered-with earth station.

The probability distribution, and the corresponding CDF of the quantized version of z (quantization interval of 0.1 dB; d_i (km)) was obtained using the proposed method and also using a commercially available simulation software. The CDF is defined here as $\text{CDF}(Z) = P(z > Z)$.

Figure 5a shows the results obtained for the probability distribution estimates with the proposed method and through a computer simulation run corresponding to 58 simulated days (1×10^6 time steps with a 5 s time step). The required computer time was around 45 min for both methods, in a 200 MHz PC machine. Fig. 5b and 5c display, in an expanded view, the regions of Fig. 5a corresponding, respectively, to lower levels of interference (side lobe interference) and higher levels of interference (close to in-line interference). It can be noted from these Figures that a good agreement between the results generated by the two methods was obtained in the range of lower levels of interference. Considering the higher levels of interference, that occur for a very a small percentage of time, we note that several values of z, although showing a positive probability in the proposed method, did not occur in the simulation results. This suggests that an increase in the number of simulated days might be required to better cover all the possibilities for the system satellites locations. These differences are also reflected in Fig. 6, which shows the obtained cumulative distribution curves in the range of higher levels of interference. Note that a difference of 1.5 dB can be observed for the values of Z corresponding to probabilities on the order of 1×10^{-4}.

FIGURE 5a

Probability distribution estimates obtained with the proposed approach and by computer simulation (58 simulated days, 5 s time step)

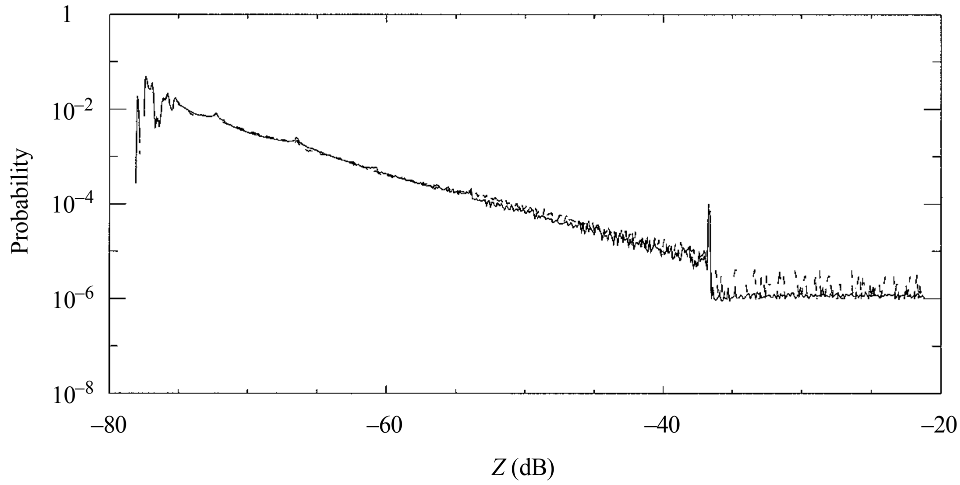

Solid line: analytical method
Dotted line: simulation

1529-05a

FIGURE 5b

Probability distribution estimates obtained with the proposed approach and by computer simulation - Lower levels of interference (58 simulated days, 5 s time step)

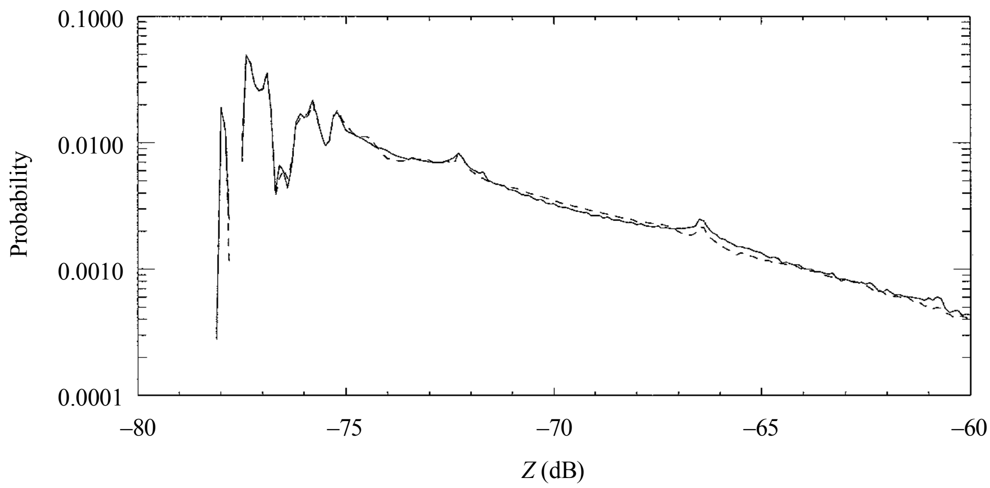

Solid line: analytical method
Dotted line: simulation

1529-05b

FIGURE 5c

Probability distribution estimates obtained with the proposed approach and by computer simulation - Higher levels of interference (58 simulated days, 5 s time step)

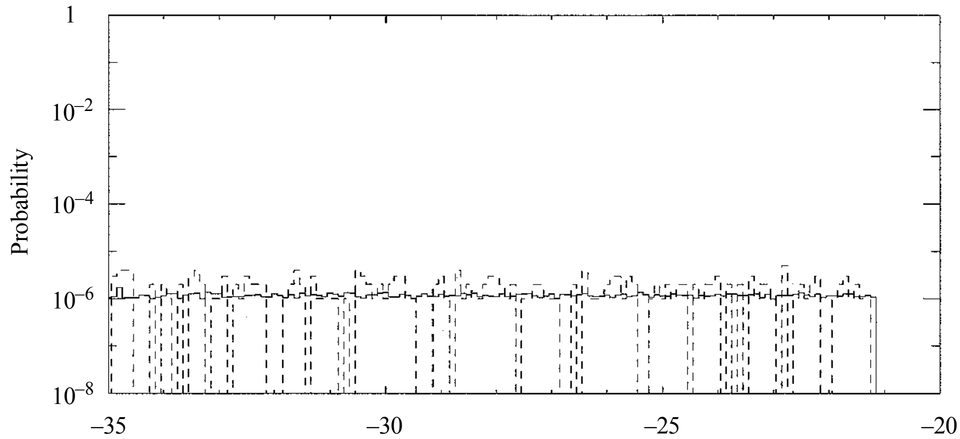

Solid line: analytical method
Dotted line: simulation

1529-05c

FIGURE 6

Cumulative distribution estimate function obtained with the proposed approach and by computer simulation - Higher levels of interference (58 simulated days, 5 s time step)

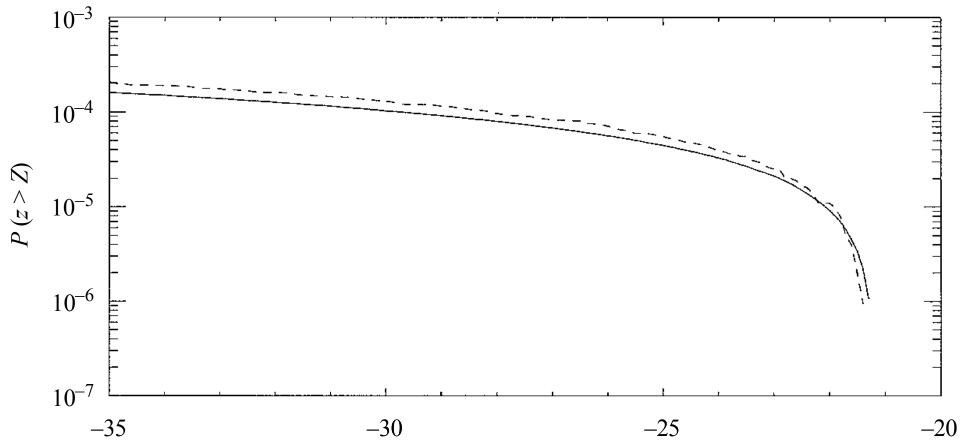

Solid line: analytical method
Dotted line: simulation

1529-06

For the simulation results shown in Fig. 7, the number of simulated days was increased from 58 to 290 and the time step was reduced from 5 to 2 s, resulting in computer simulation time of approximately 9 h and 22 min in a 200 MHz PC machine. Note the improvement in the quality of the simulation results.

FIGURE 7

Probability distribution estimates obtained with the proposed approach and by computer simulation - Higher levels of interference (290 simulated days, 2 s time step)

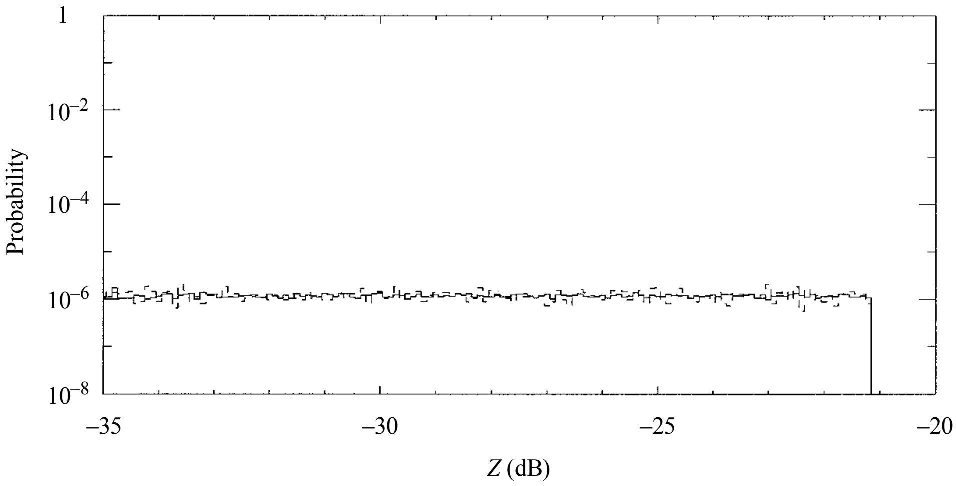

Solid line: analytical method
Dotted line: simulation

1529-07

It is worth pointing out here that, as opposed to results generated through simulation, the results obtained with the proposed analytical approach correspond to an infinite number of simulated days, and therefore, in this sense, they do not present the reliability problem associated with computer simulation methods. For a given interference environment, the computer time required by the proposed method depends on how fine is the quantization of the reference satellites φ-θ planes (similar to the size of the time step in computer simulation methods). Finer quantization trades computer time for higher precision in the numerical results. This is illustrated in Fig. 8 which shows the differences in the probability distribution estimates obtained with the proposed method when the grid element used in the non in-line interference regions of the φ-θ plane is increased from the $0.09° \times 0.09°$ square used in the previous example to a $0.15° \times 0.15°$ square, while the same size was maintained for the grid elements in the in-line interference regions. The corresponding reduction in computer time was from 45 min to around 15 min.

FIGURE 8

Probability distribution estimates obtained with the proposed approach for different grid quantizations

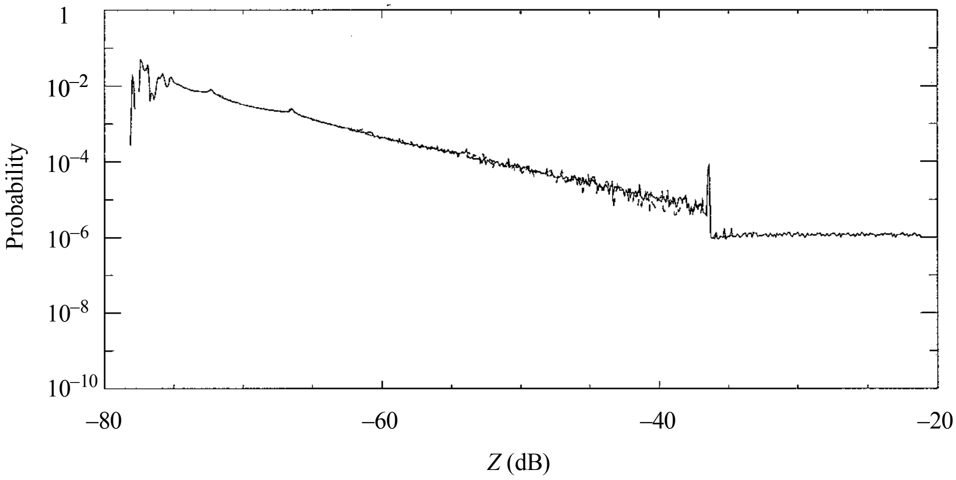

Solid line:
in-line interference region: quantization grid = 0.01° × 0.01°
non in-line interference region: quantization grid = 0.09° × 0.09°

Dotted line:
in-line interference region: quantization grid = 0.01° × 0.01°
non in-line interference region: quantization grid = 0.15° × 0.15°

1529-08

Example 2

Let us consider two non-GSO systems, LEO 1 and LEO 2. Satellite system LEO 1 has the same orbital dynamics (orbital inclination, number of planes, number of satellite per planes, altitude, etc.) as the LEO D system. Satellite system LEO 2 has the same orbital dynamics as the LEO F system. This second example considers the uplink interference from LEO 1 earth stations into a LEO 2 satellite. This situation is illustrated in Fig. 9. In this Figure, each earth station is assumed to have four antennas (beams), pointed to the LEO 1 satellites corresponding to the four highest elevation angles that satisfy the minimum elevation angle constraint (the constellation contains a total of 48 satellites). Considering that all feeder-link earth stations transmit the same power, the aggregate uplink interference power reaching a LEO 2 satellite (say, satellite i), located at a given point, is proportional to the quantity:

$$z_i = \sum_{j=0}^{N_e-1} \sum_{k=0}^{N_a-1} \frac{G_{s,i}(\alpha_{ij})\, G_{e,j}(\beta_{ijk})}{d_{ij}^2}$$

where:

$G_{s,i}(\alpha_{ij})$: receiving antenna gain of satellite i in a direction α_{ij} (degrees) off the main beam axis

$G_{e,j}(\beta_{ijk})$: earth station transmitting antenna gain in a direction β_{ijk} (degrees) off the main beam axis

d_{ij}: range between satellite i and the earth station j.

Note that the random variable z_i is a function of the given location of the considered LEO 2 interfered-with satellite and the random location of the LEO 1 reference satellite. In the equation above N_e and N_a represent, respectively, the number of earth stations and the number of antennas (per earth station) tracking a LEO 1 satellite with an elevation angle higher than the prescribed minimum value.

FIGURE 9

Uplink interference geometry

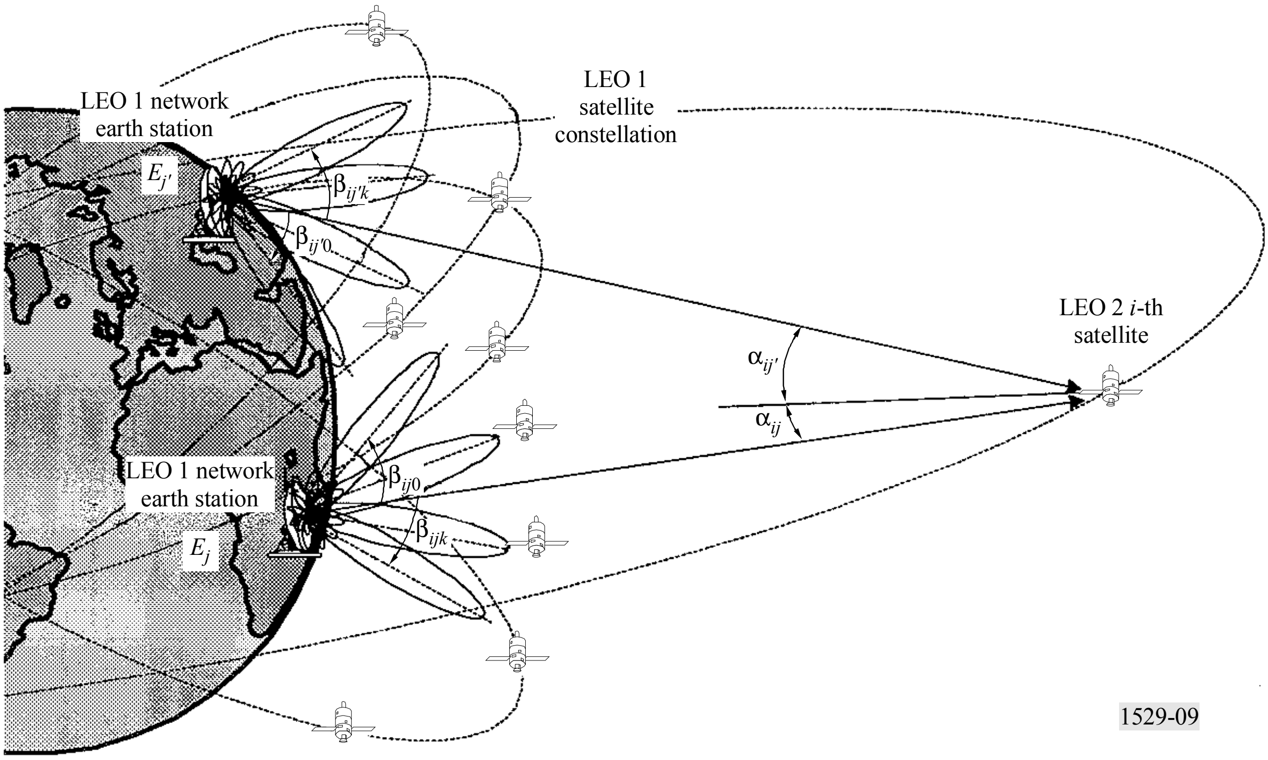

The LEO 1 earth station antenna transmitting radiation pattern was the same as in Example 1. The LEO 2 satellite receiving antenna radiation pattern was considered to have the same form as that in Example 1 but with G_{max} = 12 dBi and α_0 = 52°. The minimum operating elevation angle for the LEO 1 earth stations was assumed to be 5°. Concerning the earth station switching strategy, it was assumed that each LEO 1 gateway contains four earth station antennas that track LEO 1 satellites with elevation angles higher than the prescribed minimum value, 5°.

Results were obtained for a total of 120 LEO 1 earth stations (worldwide). The considered set of earth station locations is illustrated in Fig. 10 together with the location of the interfered-with LEO 2 satellite (black cross). The location of the LEO 2 satellite was chosen so that the number of visible earth stations is maximized (number of visible earth stations equal to 65). This way the number of interference entries to be considered is maximum.

FIGURE 10

LEO 1 earth station distribution and LEO 2 satellite location (24.5º E, 44.5º N)

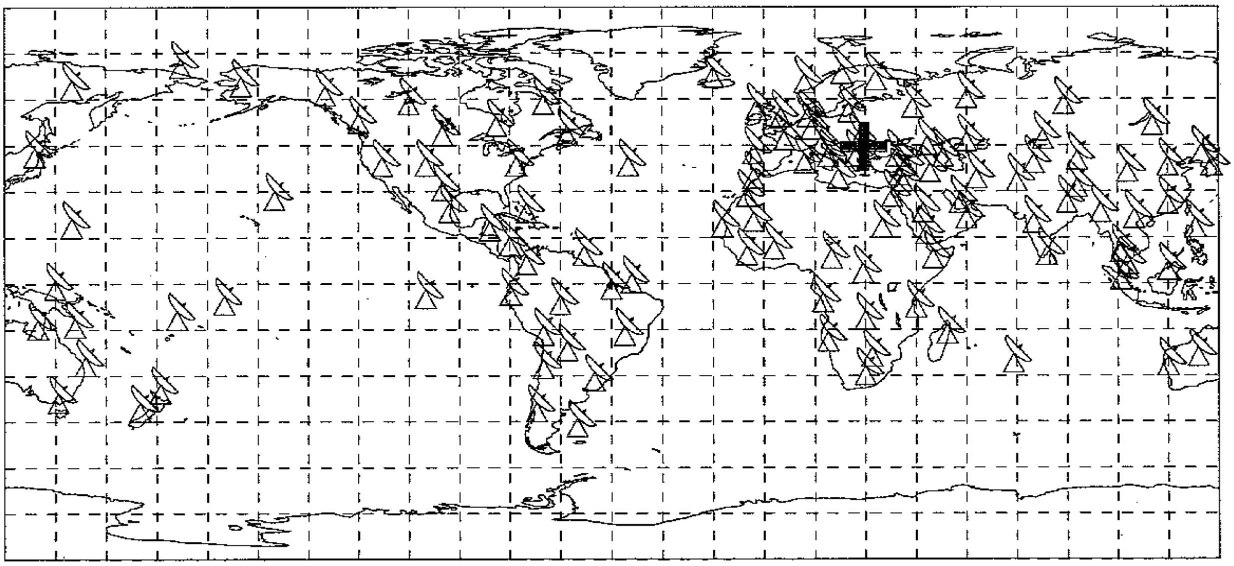

1529-10

This example illustrates the ability of the proposed analytical method to handle complex interference environment. Figure 11 illustrates the CDF obtained with the proposed approach for the variable *z*, corresponding to the aggregate uplink interference from LEO 1 earth stations into a LEO 2 satellite (120 LEO 1 earth stations worldwide). Simulation results were not obtained in this case.

FIGURE 11

Cumulative distribution estimate function obtained with the proposed approach for the variable *z*, corresponding to the aggregate uplink interference from LEO 1 earth stations into a LEO 2 satellite (120 LEO 1 earth stations worldwide)

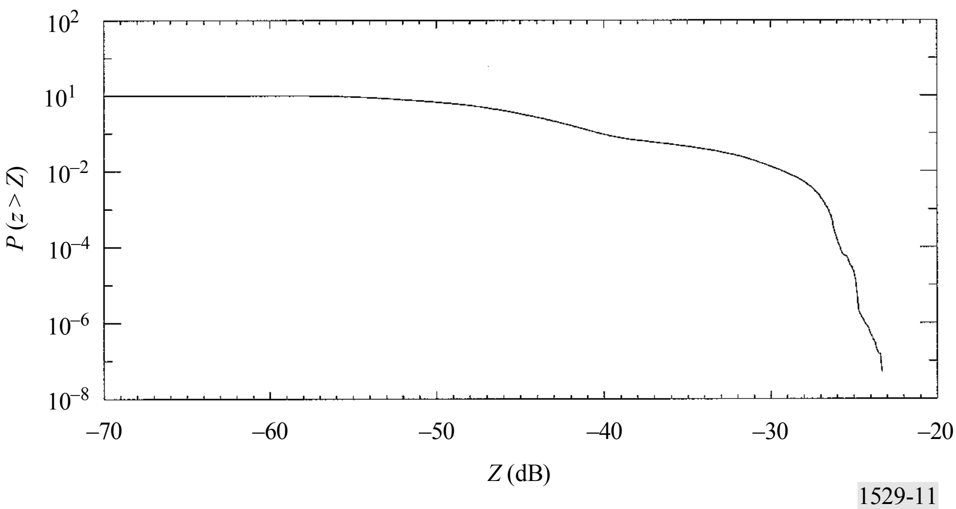

1529-11

10 Applying the analytical method to repeated track non-GSO satellite systems

When applying the methodology described in the previous sections to assess the statistical behaviour of interference when repeated track non-GSO satellite systems are involved, it is more adequate to have the position of the reference satellite given in terms of its mean anomaly M and the longitude Ω of the orbit ascending node when the satellite is at the perigee rather than in terms of its longitude and latitude, as before. In this case, the position of the reference satellite is represented by the vector $\mathbf{x} = (M, \Omega)^T, -\pi < M \leq \pi, -\pi \leq \Omega \leq \pi$. Let then $p_{\mathbf{x}}(\eta, G)$ denote the pdf function of the vector $\mathbf{x}$. Here again, the idea is to model M as a random variable and measure the probability $P(M \in \Delta)$ by the fraction of the period T (period of the satellite revolution) during which $M(t)$ takes values in the interval Δ. Under this assumption, it can be easily shown that the pdf of M is given by:

$$p_M(\eta) = \begin{cases} 1/2\pi & \text{for } -\pi < \eta \leq \pi \\ 0 & \text{otherwise} \end{cases} \tag{21}$$

On the other hand, the longitude Ω of the orbit ascending node when the satellite is at the perigee can be adequately modelled as a random variable with an uniform probability distribution in the interval $(-\pi, \pi)$ and statistically independent of M (see Appendix 1 to this Annex). In the particular case of repeated track satellites, Ω is a discrete random variable taking value in the finite set $\{\Omega_0, \Omega_1, \ldots \Omega_k, \ldots \Omega_{N-1}\}$, where Ω_k represent the longitude of successive ascending nodes (when the satellite is at the perigee) given by:

$$\Omega_k = (\Omega_0 - k\Delta\Omega_{AN})_{MOD\, 2\pi} \qquad \text{for } k = 0, \ldots, N-1 \tag{22}$$

with $\Delta\Omega_{AN}$ denoting the longitudinal spacing between successive ascending passes through the equatorial plane. The probability density function of Ω is then given by:

$$p_\Omega(G) = \sum_{k=0}^{N-1} P(\Omega = \Omega_k)\ \delta(G - \Omega_k) = \sum_{k=0}^{N-1} \frac{1}{N} \delta(G - \Omega_k) \tag{22a}$$

with $\delta(\ )$ denoting the Dirac delta function. Finally, considering equation (21) and the statistical independence of M and Ω, we have:

$$p_{\mathbf{x}}(\eta, G) = \frac{1}{2\pi} \sum_{k=0}^{N-1} \frac{1}{N} \delta(G - \Omega_k) \qquad \begin{matrix} \text{for } -\pi < \eta \leq \pi \\ -\pi < G \leq \pi \end{matrix} \tag{23}$$

Furthermore, in the particular case of repeated track satellites, the application of the analytical method involves varying the position of the reference satellite, so that all values of the pair (M, Ω) with $M \in (-\pi, \pi)$ and $\Omega \in \{\Omega_0, \Omega_1, \ldots, \Omega_{N-1}\}$ are visited. This is done by discretizing the interval $(-\pi, \pi)$ (where M takes values) into small intervals, producing, in the M-Ω plane, a set of one-dimensional cells (1-D cells) which are defined by these small intervals and any given value of $\Omega \in \{\Omega_0, \Omega_1, \ldots, \Omega_{N-1}\}$. As before, it is important to calculate the probability of finding the reference satellite inside any of these 1-D cells.

The flowchart in Fig. 12 illustrates the procedure for the application of the analytical method to repeated track satellites.

FIGURE 12

Flow chart of the analytical method (repeated track satellites)

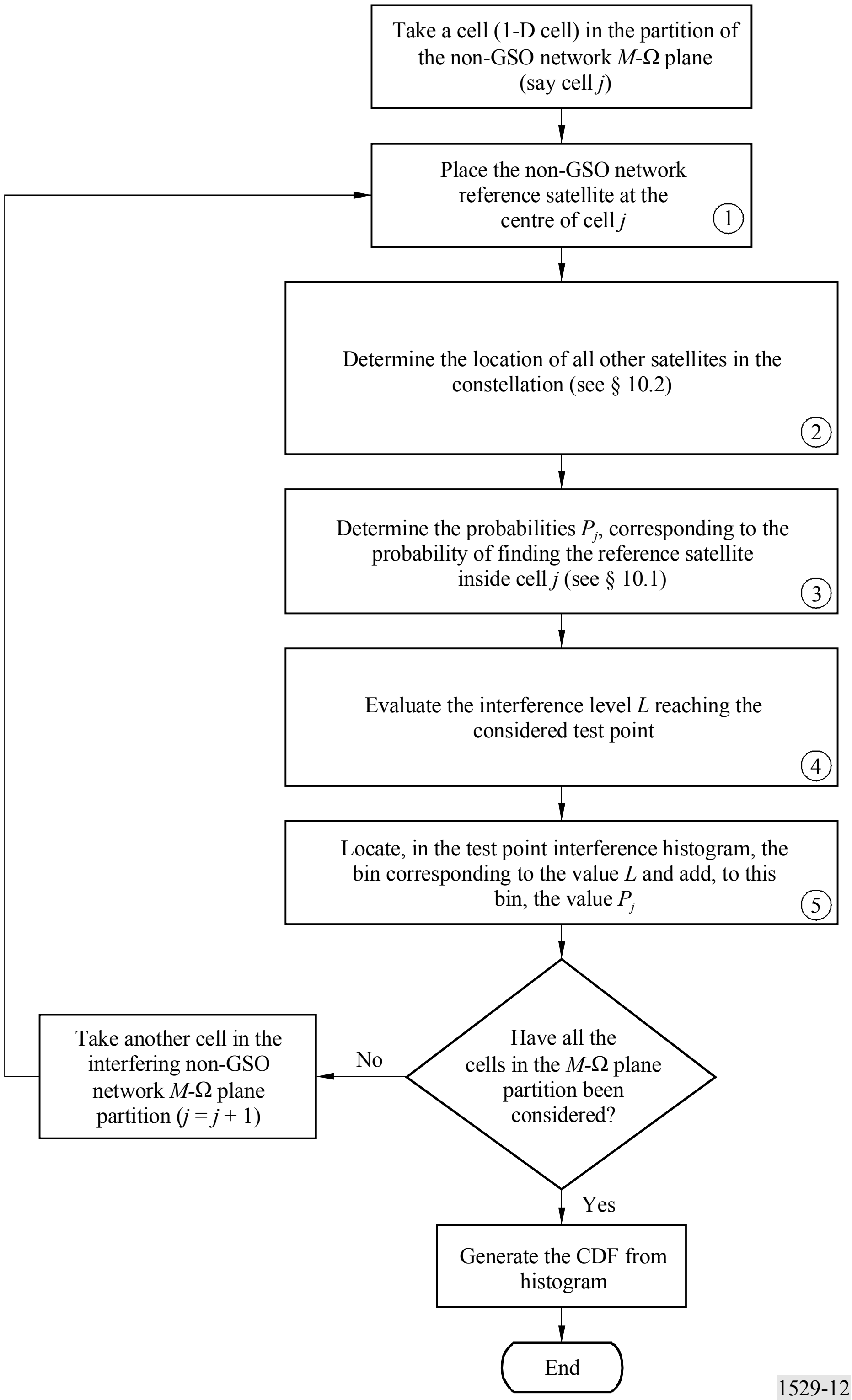

NOTE 1 – This procedure can also be applied to non-repeated track satellites. In this case, Ω is considered to be a continuous random variable, uniformly distributed over the interval (–π,π) and independent of *M* and the *M*-Ω plane is divided into small rectangular cells. The probability of finding the reference satellite inside a rectangular cell (say, cell *j*) in the *M*-Ω plane, defined by $M \in (M_m, M_M)$, $\Omega \in (\Omega_m, \Omega_M)$, can be obtained by integrating $p_{\mathbf{x}}(\eta, G)$ which, in this case, is given by:

$$p_{\mathbf{x}}(\eta, G) = \frac{1}{4\pi^2} \qquad \text{for} \quad \begin{aligned} -\pi < \eta \le \pi \\ -\pi < G \le \pi \end{aligned} \tag{24}$$

10.1 Probability of the reference satellite being inside a given cell

As mentioned before, the application of the analytical method to repeated track satellites involves varying the position of the reference satellite, so all values of the pair (M, Ω) with $M \in (-\pi,\pi)$ are visited. This is done by discretizing the interval $(-\pi,\pi)$ (where *M* takes values) into small intervals, producing, in the *M*-Ω plane, a set of one-dimensional cells (1-D cells) defined by these small intervals and any given value of $\Omega \in \{\Omega_0, \Omega_1, \ldots, \Omega_{N-1}\}$. The probability of having the reference satellite inside a given 1-D cell (say, cell *j*) defined, for example, by the points in the *M*-Ω plane satisfying the condition $\{M_m < M \le M_M,\ \Omega = \Omega_i\}$ can be determined from equation (23) and is given by:

$$P_j = P(M_m < M \le M_M,\ \Omega = \Omega_i) = \frac{M_M - M_m}{2\pi N} \qquad \text{for } i = 1, \ldots, N \tag{25}$$

NOTE 1 – As mentioned before, it is also possible to apply this technique to non-repeated track satellites. In this case, Ω is considered to be a continuous random variable, uniformly distributed over the interval (–π,π) and independent of *M*. The *M*-Ω plane is then divided into small rectangular cells. The probability of finding the reference satellite inside a rectangular cell in the *M*-Ω plane (say cell *j*), defined by $M \in (M_m, M_M)$, $\Omega \in (\Omega_m, \Omega_M)$, can be obtained from equation (24) and is given by:

$$P_j = P(M_m < M \le M_M,\ \Omega_m < \Omega \le \Omega_M) = \frac{(M_M - M_m)(\Omega_M - \Omega_m)}{4\pi^2} \tag{26}$$

10.2 Finding the position of all satellites in the constellation

This section uses the same notation as that in Section 5. Let $\mathbf{x} = (M, \Omega)^T$ be the vector characterizing the position of the reference satellite. Since, in this case, the mean anomaly of the reference satellite is know (not the latitude as before), there is only one constellation configuration associated with the pair (M, Ω). To determine the positions of all other satellites in the constellation configuration, the following quantities have to be calculated for, $i = 0, \ldots, N_{Satperplane} - 1$ and $j = 0, \ldots, N_{Planes} - 1$:

$$M_i^j = M + i\beta + j\lambda \tag{27}$$

$$E_i^j = M_i^j + 2\sum_{n=1}^{\infty} \frac{1}{n} J_n(ne)\sin(nM_i^j) \tag{28}$$

$$\upsilon_i^j = 2\arctan\left(k \tan\frac{E_i^j}{2}\right) \tag{29}$$

$$r_i^j = \frac{a(1-e^2)}{1-e\cos(\upsilon_i^j)} \tag{30}$$

$$\gamma_i^j = (\upsilon_i^j + \omega)_{MOD\,2\pi} \tag{31}$$

$$\theta_i^j = \arcsin\left(\sin\delta\sin(\gamma_i^j)\right) = f_1(\gamma_i^j) \tag{32}$$

$$\varphi_{s_i}^{\;j} = \arccos\left[\frac{\cos(\gamma_i^j)}{\cos(f_1(\gamma_i^j))}\right]\mathrm{sgn}(\gamma_i^j) \tag{33}$$

$$\varphi_i^j = (\varphi_{s_i}^{\;j} + \Omega_g + j\psi)_{MOD\,2\pi} \tag{34}$$

In the above expression, Ω_g denotes the longitude of the ascending node corresponding to the reference satellite orbital plane, which can be written in terms of the longitude Ω of the ascending node when the reference satellite is at the perigee and the reference satellite mean anomaly M, as:

$$\Omega_g = (\Omega - M\Delta\Omega_{AN} / 2\pi)_{MOD\,2\pi} \tag{35}$$

with $\Delta\Omega_{AN}$ denoting the longitudinal spacing between successive ascending passes through the equatorial plane. Note that, as expected, when the reference satellite is at the perigee, $M = 0$ and, consequently $\Omega_g = \Omega$.

Finally, the vector defining the position of the i-th satellite in the j-th plane is given by:

$$\mathbf{p}_i^j = \begin{pmatrix} r_i^j\cos(\theta_i^j)\cos(\varphi_i^j) \\ r_i^j\cos(\theta_i^j)\sin(\varphi_i^j) \\ r_i^j\sin(\theta_i^j) \end{pmatrix} \tag{36}$$

10.3 Choosing the mean anomaly increments

The value of the mean anomaly increment ΔM depends on the value of the true anomaly increments $\Delta\upsilon$, which are chosen according to the same criteria as those presented in Section 6 for choosing longitude and latitude increments. Considering the non-linear relationship between the mean anomaly and the true anomaly, it can be easily shown that if an uniform quantization of the mean anomaly is desired, the mean anomaly increment shall satisfy the inequality:

$$\frac{\Delta M}{\Delta\upsilon} \le \min_{\upsilon}\frac{dM}{d\upsilon} = \frac{1-e}{k} \tag{37}$$

where $\Delta\upsilon$ represents the required (maximum) true anomaly increment.

NOTE 1 – For non-repeated track satellites, in which case Ω is considered to be a continuous random variable, uniformly distributed over the interval $(-\pi,\pi)$ and independent of M, the increments $\Delta\Omega$ are to be chosen according to the same criteria as those presented in Section 6 for choosing longitude and latitude increments.

10.4 Comments

The following observations can be made, concerning the procedure in Section 10:

– The procedure can be also applied to non-repeated track satellites, in which case Ω is modelled as a uniformly distributed random variable over the interval $(-\pi,\pi)$.

– By working in the M-Ω plane, it is possible to take advantage of some symmetry that may exist in the satellite constellation, thus reducing the computation time. In this case, it may be advantageous to work in the M-Ω_g plane rather then the M-Ω plane. Note that, in the case of repeated track satellites, M and Ω_g are not statistically independent random variables. In fact, from equations (23) and (35) we have:

$$p_{\Omega_g|M=\eta}(G) = \sum_{k=0}^{N-1} \frac{1}{N} \delta\left(G - (\Omega_k - \frac{\eta \Delta\Omega_{AN}}{2\pi})_{MOD\,2\pi} \right)$$

and, additionally considering equation (21):

$$p_{M\Omega_g}(\eta, G) = \frac{1}{2\pi} \sum_{k=0}^{N-1} \frac{1}{N} \delta\left(G - (\Omega_k - \frac{\eta \Delta\Omega_{AN}}{2\pi})_{MOD\,2\pi} \right) \qquad \text{for} \quad \begin{array}{l} -\pi < \eta \le \pi \\ -\pi < G \le \pi \end{array}$$

In the case of non repeated track satellites, considering equation (35) and the fact that Ω is uniformly distributed in $(-\pi,\pi)$ and statistically independent of M, it can be shown that Ω_g is also uniformly distributed in $(-\pi,\pi)$ and statistically independent of M. In this case:

$$p_{M\Omega_g}(\eta, G) = \frac{1}{4\pi^2} \qquad \text{for} \quad \begin{array}{l} -\pi < \eta \le \pi \\ -\pi < G \le \pi \end{array}$$

– Working in the M-Ω plane or in the M-Ω_g planes requires a larger number of cells then working in φ-θ plane. In fact, the cells of the φ-θ plane are visited more than one time (at least twice). In particular, cells of the φ-θ plane that have latitude close to the maximum value δ are visited many times.

– The **PPII** and **RPII** concepts described in Sections 3, 6 and 7 (aiming the joint use of fine and coarse quantization grids) can be also implemented. In this case the **PPII**s have to be determined in the φ-θ plane and then transferred to the M-Ω plane, where the **RPII**s are defined.

APPENDIX 1

TO ANNEX 1

pdf of the position of a non-GSO satellite

To obtain an analytical expression for the pdf $p_{\mathbf{x}}(\Phi,\Theta)$ of the position $\mathbf{x}$ of a non-GSO satellite, let us consider first the orientation of an elliptical Earth orbit, illustrated in Fig. 13. In this Figure, the inclination δ is the angle between the plane of the orbit and the equatorial plane. The right ascension of the ascending node (RAAN) Ω is measured eastward from the vernal equinox, defining the orientation of the orbit plane. The argument of the perigee ω defines the orientation of the elliptical orbit within the orbital plane. The angle γ represents the angular displacement of the satellite measured from the line of nodes (intersection of the equatorial plane and the orbit plane) and is given by:

$$\gamma = (\omega + \upsilon)_{MOD\,2\pi} \tag{38}$$

with υ denoting the so-called true anomaly associated to the satellite position. In this reference system, given δ and the RAAN Ω, the satellite position is characterized by its distance r to the centre of the Earth and the angular displacement γ. Throughout this Appendix, $(x)_{MOD\,2\pi}$ takes values in the interval $(-\pi, \pi)$.

FIGURE 13

Orientation of an elliptical Earth orbit

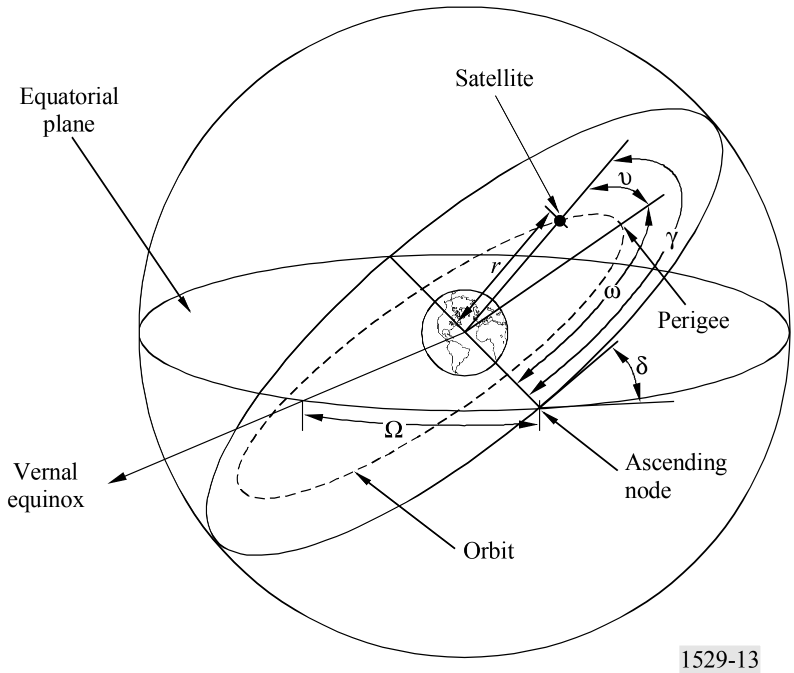

As shown later in this section, the desired pdf $p_{\mathbf{x}}(\Phi, \Theta)$ can be obtained from pdf $p_\gamma(\Gamma)$ of γ. To derive $p_\gamma(\Gamma)$, we first note that the angular displacement γ, given by equation (38) can be expressed in terms of the so called eccentric anomaly angle E as:

$$\gamma = \left(\omega + 2 \arctan \left[k \tan\left(\frac{E}{2} \right) \right] \right)_{MOD\,2\pi} \tag{39}$$

where:

$$k = \sqrt{\frac{1+e}{1-e}} \tag{40}$$

with e denoting the orbit eccentricity. It is also known that the satellite eccentric anomaly E satisfies the Kepler equation:

$$M_0 + \frac{2\pi}{T}(t - t_e) = E - e\sin(E) \tag{41}$$

The left-hand side of equation (41) corresponds to the satellite mean anomaly M, with M_0 denoting its value at a reference time t_e and T the period of the satellite revolution. The eccentric anomaly E is a periodic function with period T. The approach here is to model E as a random variable and measure the probability $P(E \in \Delta)$ by the fraction of the period T during which $E(t)$ takes values in the interval Δ. This is equivalent to consider, in equation (41), that t is a random variable uniformly distributed in $(0, T)$. This assumption establishes a correspondence between percentage of time and probability, guaranteeing that the results obtained with the analytical method correspond to those that would be obtained through time simulation methods in an infinite simulation time. From these assumptions and the relationship in equation (41) it is possible to determine the pdf of E which, for E defined modulo 2π, is given by:

$$p_E(\varepsilon) = \begin{cases} \dfrac{1 - e\cos(\varepsilon)}{2\pi} & \text{for } \; -\pi < \varepsilon \le \pi \\ 0 & \text{otherwise} \end{cases} \tag{42}$$

In the same way, using equation (42) and the relationship in equation (39), the pdf of γ was derived, and is given by:

$$p_\gamma(\Gamma) = \begin{cases} \dfrac{k(1+e)}{2\pi} \left[\dfrac{1 + \tan^2\left(\dfrac{\Gamma - \omega}{2}\right)}{k^2 + \tan^2\left(\dfrac{\Gamma - \omega}{2}\right)} \right]^2 & \text{for } \; -\pi < \Gamma \le \pi \\ 0 & \text{otherwise} \end{cases} \tag{43}$$

To determine $p_{\mathbf{X}}(\Phi, \Theta)$ it is necessary to consider the position of the satellite in a geostationary reference system, as illustrated in Fig. 14. In this Figure, the satellite is located at the position P having latitude θ and longitude φ given by:

$$\varphi = (\varphi_s + \Omega_g)_{MOD\, 2\pi} \tag{44}$$

with φ_s being the longitude variation due to the angular displacement γ and Ω_g the longitude of the line of nodes, which changes with the Earth's rotation movement and with the nodal regression of the ascending node. The longitude the line of nodes Ω_g can be written as:

$$\Omega_g = \left(\Omega_0 + (\Omega_e + \Omega_r)t\right)_{MOD\, 2\pi} \tag{45}$$

where Ω_0 is the longitude of the line of nodes at the initial time and Ω_e and Ω_r are, respectively, the Earth angular velocity and the angular regression of the ascending node. Considering that both angular velocities Ω_e and Ω_r are constant, the longitude Ω_g can be adequately modelled as a random variable uniformly distributed in $(-\pi, \pi)$.

To express φ_s and θ as functions of γ, consider the geometry in Fig. 14. From this Figure it is easy to conclude that:

$$\overline{OP}\sin(\theta) = \overline{OP}\sin(\gamma)\sin(\delta) \tag{46}$$

$$\overline{OP}\cos(\gamma) = \overline{OP}\cos(\theta)\cos(\varphi_s) \tag{47}$$

or,

$$\sin(\theta) = \sin(\gamma)\,\sin(\delta) \tag{48}$$

$$\cos(\gamma) = \cos(\theta)\,\cos(\varphi_s) \tag{49}$$

FIGURE 14

Problem geometry

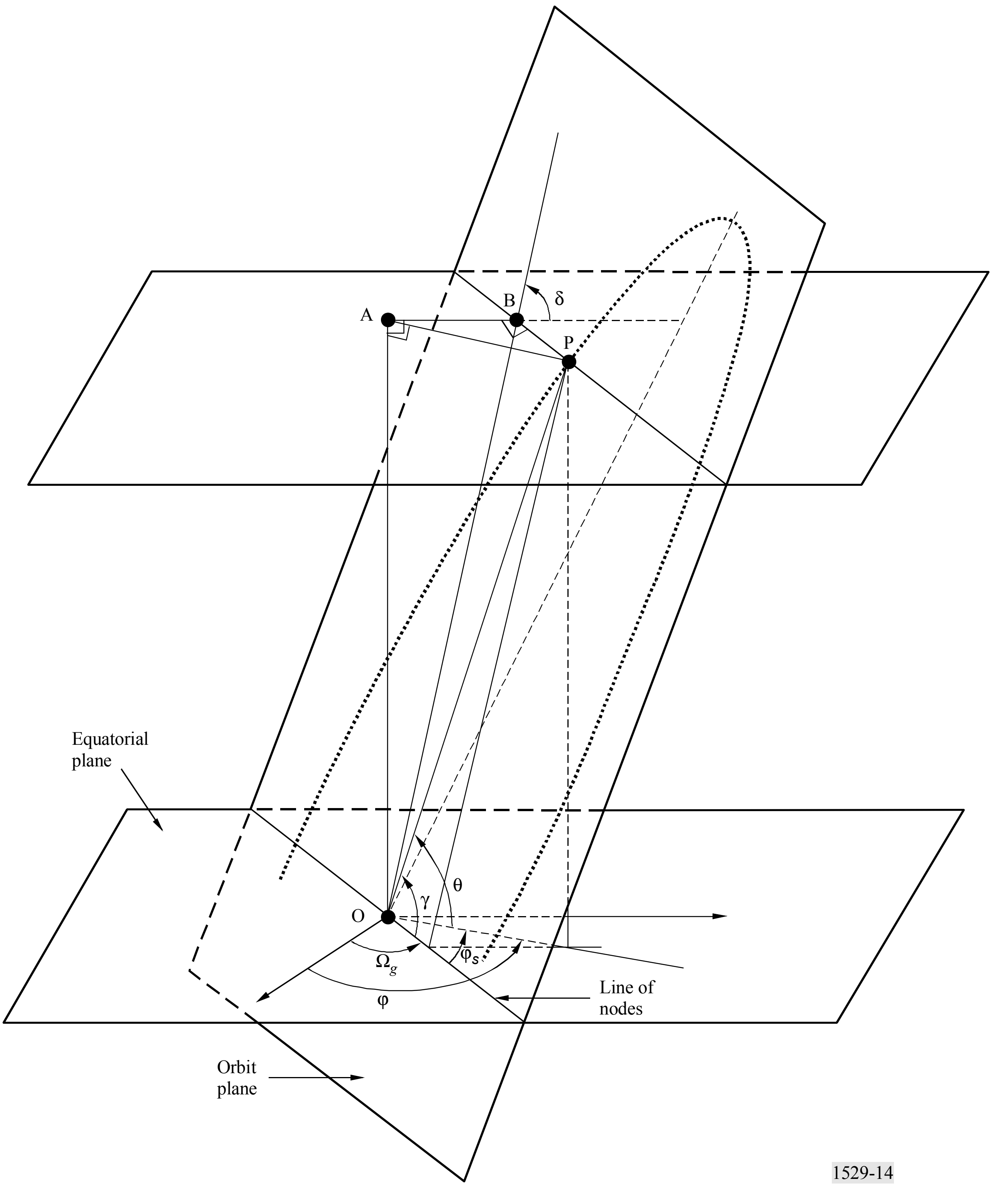

From equation (48), we have:

$$\theta = \arcsin(\sin\delta \sin\gamma) = f_1(\gamma) \tag{50}$$

and from equation (49), taking equation (50) into consideration,

$$\varphi_s = \arccos\left[\frac{\cos\gamma}{\cos(f_1(\gamma))}\right]\operatorname{sgn}(\gamma) = f_2(\gamma) \tag{51}$$

with sgn( ) representing the signum function, which was included to extend the validity of the equality to the range $\gamma \in (-\pi, \pi)$.

Furthermore, considering equation (44) and equation (51), we have:

$$\varphi = (\varphi_s + \Omega_g)_{MOD\,2\pi} = (f_2(\gamma) + \Omega_g)_{MOD\,2\pi} \tag{52}$$

Assuming that the line of nodes longitude Ω_g and the angular displacement γ are statistically independent random variables, and since Ω_g is uniformly distributed in $(-\pi, \pi)$, it can be shown that the random variable φ is also uniformly distributed in $(-\pi, \pi)$ for any given value of γ, that is:

$$p_{\varphi|\gamma=\Gamma}(\Phi) = p_\varphi(\Phi) = \begin{cases} \dfrac{1}{2\pi} & \text{for } -\pi < \Phi \le \pi \\ 0 & \text{otherwise} \end{cases} \tag{53}$$

Note now that, being statistically independent of γ, φ is also statistically independent of $\theta = f_1(\gamma)$. Therefore the pdf of the position **x** of the non-GSO satellite can be written as:

$$p_{\mathbf{x}}(\Phi, \Theta) = p_\varphi(\Phi)\, p_\theta(\Theta) \tag{54}$$

The pdf $p_\theta(\Theta)$ of the latitude Θ, can be obtained using equation (50) and considering that $p_\gamma(\Gamma)$ is given by equation (43). It then results:

$$p_\theta(\Theta) = p_{\theta|AM}(\Theta) P(AM) + p_{\theta|DM}(\Theta) P(DM) \tag{55}$$

where $p_{\theta|AM}(\Theta)$ and $p_{\theta|DM}(\Theta)$ are the pdf of the satellite latitude given that the satellite is in ascending and descending mode, respectively. These conditional pdf's are given by:

$$p_{\theta|AM}(\Theta) = \begin{cases} \dfrac{1}{P(AM)} \dfrac{k(1+e)}{2\pi} \dfrac{\cos\Theta}{\sqrt{\sin^2\delta - \sin^2\Theta}} \left[\dfrac{2\sin\delta}{(1+k^2)\sin\delta - (1-k^2)g(\Theta)}\right]^2 & \text{for } -\delta < \Theta \le \delta \\ 0 & \text{otherwise} \end{cases} \tag{56}$$

and

$$p_{\theta|DM}(\Theta) = \begin{cases} \dfrac{1}{P(DM)} \dfrac{k(1+e)}{2\pi} \dfrac{\cos\Theta}{\sqrt{\sin^2\delta - \sin^2\Theta}} \left[\dfrac{2\sin\delta}{(1+k^2)\sin\delta + (1-k^2)g(-\Theta)}\right]^2 & \text{for } -\delta < \Theta \le \delta \\ 0 & \text{otherwise} \end{cases} \tag{57}$$

with $P(AM)$ and $P(DM)$ denoting, respectively, the probability of the satellite being in ascending and descending mode, which are given by:

$$P(AM) = \int_{-\delta}^{\delta} \frac{k(1+e)}{2\pi} \frac{\cos\Theta}{\sqrt{\sin^2\delta - \sin^2\Theta}} \left[\frac{2\sin\delta}{(1+k^2)\sin\delta - (1-k^2)g(\Theta)}\right]^2 \mathrm{d}\Theta \tag{58}$$

and

$$P(DM) = \int_{-\delta}^{\delta} \frac{k(1+e)}{2\pi} \frac{\cos\Theta}{\sqrt{\sin^2\delta - \sin^2\Theta}} \left[\frac{2\sin\delta}{(1+k^2)\sin\delta + (1-k^2)g(-\Theta)}\right]^2 \mathrm{d}\Theta \tag{59}$$

If the integrals in equations (58) and (59) are performed, we have:

$$P(AM) = h(\omega) - h(-\omega) \tag{60}$$

$$P(DM) = h(\pi-\omega) - h(-\pi+\omega) \tag{61}$$

where:

$$h(\omega) = \frac{1}{\pi}\arctan\left(\frac{\alpha(\omega)}{k}\right) - \frac{ke}{\pi}\left(\frac{\alpha(\omega)}{\alpha^2(\omega)+k^2}\right) + \frac{1+\mathrm{sgn}(\omega-\pi/2)}{2} \tag{62}$$

with:

$$\alpha(\omega) = \frac{1-\sin\omega}{\cos\omega} \tag{63}$$

In equations (57) to (59),

$$g(\Theta) = \cos\omega\sqrt{\sin^2\delta - \sin^2\Theta} + \sin\omega\sin\Theta \tag{64}$$

and k is given by equation (40).

Finally, from equations (54), (53) and (55) to (59), we have:

$$p_{\mathbf{x}}(\Phi,\Theta) = p_{\mathbf{x}|AM}(\Phi,\Theta)P(AM) + p_{\mathbf{x}|DM}(\Phi,\Theta)P(DM) \tag{65}$$

where $p_{\mathbf{x}|AM}(\Phi,\Theta)$ and $p_{\mathbf{x}|DM}(\Phi,\Theta)$ are the pdf's of the satellite position (longitude and latitude) given that the satellite is in ascending and descending mode, respectively. These conditional pdf's are given by:

$$p_{\mathbf{x}|AM}(\Phi,\Theta) = \begin{cases} \dfrac{1}{P(AM)} \dfrac{k(1+e)}{4\pi^2} \dfrac{\cos\Theta}{\sqrt{\sin^2\delta - \sin^2\Theta}} \left[\dfrac{2\sin\delta}{(1+k^2)\sin\delta - (1-k^2)g(\Theta)}\right]^2 & \text{for } -\delta < \Theta \le \delta,\ -\pi < \Phi \le \pi \\ 0 & \text{otherwise} \end{cases} \tag{66}$$

and

$$p_{\mathbf{x}|DM}(\Phi,\Theta) = \begin{cases} \dfrac{1}{P(DM)} \dfrac{k(1+e)}{4\pi^2} \dfrac{\cos\Theta}{\sqrt{\sin^2\delta - \sin^2\Theta}} \left[\dfrac{2\sin\delta}{(1+k^2)\sin\delta + (1-k^2)g(-\Theta)}\right]^2 & \text{for } -\delta < \Theta \le \delta,\ -\pi < \Phi \le \pi \\ 0 & \text{otherwise} \end{cases} \tag{67}$$

Alternatively, equation (65) can be written as:

$$p_{\mathbf{x}}(\Phi,\Theta)=\begin{cases}\dfrac{k(1+e)}{4\pi^2}\dfrac{\cos\Theta}{\sqrt{\sin^2\delta-\sin^2\Theta}}\left[\left(\dfrac{2\sin\delta}{(1+k)\sin\delta-(1-k^2)g(\Theta)}\right)^2+\left(\dfrac{2\sin\delta}{(1+k)\sin\delta+(1-k^2)g(-\Theta)}\right)^2\right] & \text{for } -\delta<\Theta\leq\delta \\ & \quad -\pi<\Phi\leq\pi \\ 0 & \text{otherwise}\end{cases} \tag{68}$$

In the particular case of circular orbits $(e=0\rightarrow k=1)$, equations (66) and (67) are reduced to:

$$p_{\mathbf{x}|AM}(\Phi,\Theta)=p_{\mathbf{x}|DM}(\Phi,\Theta)=\begin{cases}\dfrac{1}{2\pi^2}\dfrac{\cos\Theta}{\sqrt{\sin^2\delta-\sin^2\Theta}} & \text{for } -\delta<\Theta\leq\delta \\ & \quad -\pi<\Phi\leq\pi \\ 0 & \text{otherwise}\end{cases} \tag{69}$$

Note that in obtaining (69) it was considered that:

$$P(AM)=P(DM)=\frac{1}{2}$$

Consequently:

$$p_{\mathbf{x}}(\Phi,\Theta)=\begin{cases}\dfrac{1}{2\pi^2}\dfrac{\cos(\Theta)}{\sqrt{\sin^2\delta-\sin^2\Theta}} & \text{for } -\delta<\Theta<\delta \\ & \quad -\pi<\Phi\leq\pi \\ 0 & \text{otherwise}\end{cases} \tag{70}$$

Expressions (68) and (70) can be used, for example, to determine the probability of having a satellite in any given regions of the sky.

They also produce pdf’s such as the one examplified shown in Fig. 2.